Pergamon

Mechanics Research Communications, Vol. 28, No. 6, pp. 637–651, 2001

0093-6413/01/$–see front matter

PII: S0093-6413(02)00216-1

COUPLED THERMOMECHANICAL DYNAMICS OF PHASE TRANSITIONS IN SHAPE MEMORY ALLOYS AND RELATED HYSTERESIS PHENOMENA

R. V. N. Melnik
University of Southern Denmark, Mads Clausen Institute,
Sonderborg,DK-6400, Denmark, E-mail: rmelnik@mci.sdu.dk

A. J. Roberts and K. A. Thomas
Department of Mathematics and Computing
University of Southern Queensland, QLD 4350, Australia

(Received 2 April 2001: accepted for print 17 November 2001)

Abstract

In this paper the nonlinear dynamics of shape memory alloy phase transformations is studied with thermomechanical models based on coupled systems of partial differential equations by using computer algebra tools. The reduction procedures of the original model to a system of differential-algebraic equations and its solution are based on the general methodology developed by the authors for the analysis of phase transformations in shape memory materials with low dimensional approximations derived from center manifold theory. Results of computational experiments revealing the martensitic-austenitic phase transition mechanism in a shape-memory-alloy rod are presented. Several groups of computational experiments are reported. They include results on stress- and temperature-induced phase transformations as well as the analysis of the hysteresis phenomenon. All computational experiments are presented for Cu-based structures.

1. Introduction

A better understanding of the dynamics of phase transitions in shape memory alloys (SMA) is important for many areas of applications ranging from domestic appliances, automotive industry to bioengineering and aerospace industry [1]. However, the analysis of this dynamics requires dealing with challenging applied mechanics and mathematics problems, ones of the most difficult in nonlinear wave theory [2]. In addition to a strong nonlinear coupling of mechanical and thermal fields, intrinsic to this dynamics, in many applications

one also has to deal with various types of dynamic loadings (in particular, where these materials are used in various passive and active vibration isolation systems such as absorbers or vibration dampers, in creating dynamic response control elements, hybrid devices where they are embedded, e.g., in a resin epoxy matrix, etc). As a result, strongly nonlinear behaviour of these materials with complex phase transformations observed at the macroscopic level requires quite sophisticated models based on coupled systems of partial differential equations (PDE) and efficient numerical tools for their solution. What is also important to note is that such models are under continuous scrutiny of scientists and therefore they undergo continuous improvements by incorporating new details into PDE-based models describing the thermomechanical field of these materials (e.g., via better approximations of the free energy function, new constitutive models etc). Under these circumstances it is important to develop a general strategy of studying the dynamics of SMA as well as a methodology for the model improvement. Such a methodology has been proposed in recent authors' papers [3, 4, 5]. It has been argued that centre manifold approximations (e.g., [5]) of complicated models for SMA provide a *systematic* approach to the study of shape memory alloys dynamics. The purpose of this paper is to demonstrate that the strategy developed for the solution of resulting low-dimensional models provides a powerful tool in capturing all main features of complicated dynamics of phase transformations in SMA and related hysteresis phenomena. The model chosen in this paper as the "battle horse" has been derived from the Landau-Devonshire phenomenology and the Cattaneo-Vernotte model.

The dynamics of martensitic-austenitic transformations has been investigated experimentally in a wide range of materials, in particular in metallic alloys such as NiTi, CuZnAl, CuZnGa, CuZn, NiAl, CuAlNi, and AgCd. Subject to appropriate thermomechanical conditions, these dynamics often exhibit a hysteretic behaviour accompanied by shape-memory effects. For example, if an unstressed shape-memory-alloy wire has been stretched at low temperature, it can be returned to its initial condition upon heating. Upon cooling it can be again returned to its stretched form. In other words, the materials under consideration can be "imprinted" with a shape that they "remember". Not surprisingly these effects have a wide variety of applications ranging from heat engines and different types of actuators to robotics, oceanographic and aerospace industries, and over recent years, the interest in modelling the dynamics of shape-memory-alloys has been dramatically increased. This includes experimental [6], theoretical [7, 8, 9], and computational works [10, 11, 12]. Current and emerging applications of shape memory alloys require a deeper understanding of structural phase transitions in solids and provide new challenging problems in applied mechanics and mathematics.

Many smart materials display a strong dependence of load deformation upon temperature. Therefore, in order to adequately model the dynamics of these materials it is important to account for the coupling of stresses, deformation gradients and displacements to the thermal field. Such a coupling is critical in the description of many phenomena that are becoming increasingly important in a wide range of applications of smart materials and structures. The strong nonlinear coupling between thermal and mechanical fields provides an important key to a better understanding of hysteresis-type phenomena. Since these phenomena and the associated shape-memory effects are very difficult to control experimentally, the tools of mathematical modelling and computational experiment play an increasing role in the investigation of thermally and mechanically induced hysteresis in viscoelastic and pseudoplastic materials.

Our main focus in this paper is the adequate description of thermomechanical behaviour

of a large shape-memory-alloy rod in the martensitic-austenitic phase transition. Since the description of the mechanism of this transition requires nonconvex free energy functions, this leads to serious modelling difficulties even in low-dimensional cases. In this paper we present several groups of computational experiments aimed at the analysis of phase transition dynamics and related hysteresis phenomena in shape memory alloys. In particular, we investigate the mechanical control of phase transitions in shape-memory-alloys where phase transitions are activated by applied stresses at the body boundary. We also investigate thermally induced phase transitions and demonstrate the combined effect of distributed heating and boundary stresses on the development of phase transformations. Finally, we present computational results on and the analysis of hysteresis phenomena for different types of thermomechanical conditions.

We organised the rest of this paper as follows. In Section 2 we discuss mechanisms for thermomechanical coupling in models describing SMA dynamics and formulate the model used as the basis for our analysis in this paper. In Section 3 we provide the reader with the main ideas of our numerical approximations. The main part of the paper is Section 4, where we report computational results from the investigation of martensitic-austenitic phase transitions and thermally induced hystereses. Finally, in Section 5 we discuss future directions of the presented work.

2. Coupling Mechanisms Between Thermal and Mechanical Fields in Mathematical Models for Shape Memory Alloy Dynamics

In order to derive a basic model for SMA dynamics for which our methodology will be demonstrated we follow the Landau-Devonshire phenomenology [13, 14] and use the Cattaneo-Vernotte model for relating the heat flux and temperature. This leads us to the equations of motion and energy balance in the following form [4]:

$$\begin{cases} C_v\left[\dfrac{\partial\theta}{\partial t}+\tau_0\dfrac{\partial^2\theta}{\partial t^2}\right]-k_1\left[\theta\dfrac{\partial u}{\partial x}\dfrac{\partial^2 u}{\partial t\partial x}+\tau_0\dfrac{\partial}{\partial t}\left(\theta\dfrac{\partial u}{\partial x}\dfrac{\partial^2 u}{\partial t\partial x}\right)\right]-\mu\left[\left(\dfrac{\partial^2 u}{\partial t\partial x}\right)^2+\right. \\ \left.\tau_0\dfrac{\partial}{\partial t}\left(\dfrac{\partial^2 u}{\partial t\partial x}\right)^2\right]-\nu\left[\dfrac{\partial\theta}{\partial t}\dfrac{\partial^2 u}{\partial t\partial x}+\tau_0\dfrac{\partial}{\partial t}\left(\dfrac{\partial\theta}{\partial t}\dfrac{\partial^2 u}{\partial t\partial x}\right)\right]-\dfrac{\partial}{\partial x}\left(k\dfrac{\partial\theta}{\partial x}\right)=G\,, \\ \rho\dfrac{\partial^2 u}{\partial t^2}-\dfrac{\partial}{\partial x}\left[k_1\dfrac{\partial u}{\partial x}(\theta-\theta_1)-k_2\left(\dfrac{\partial u}{\partial x}\right)^3+k_3\left(\dfrac{\partial u}{\partial x}\right)^5\right]-\mu\dfrac{\partial^3 u}{\partial x^2\partial t}-\nu\dfrac{\partial^2\theta}{\partial x\partial t}=F\,, \end{cases} \tag{1}$$

where u is the displacement field, θ is the temperature field, τ_0 is the thermal relaxation time, k is the thermal conductivity of the material, C_v is the specific heat constant of the material, μ and ν are material-specific coefficients that characterise the dependency of the stress on the rate of the deformation gradient and temperature respectively, ρ is the density of the material, θ_1 is a positive constant that characterises a critical temperature of the material, and k_i, $i=1,2,3$ are material-specific constants that characterise the material's free energy. The right-hand side parts of system (1), F and G, represent the distributed mechanical and thermal loadings of the body. System (1) is completed by appropriate initial and boundary conditions and has to be solved with respect to (u,θ) in the spatial-temporal region $Q=\{(x,t): 0\le x\le L,\quad 0\le t\le T_f\}$, where L is the length of the structure and T_f

is the required time of observation. The initial conditions for the model (1) are taken in the following form

$$u(x,0) = u^0(x), \quad v(x,0) = \frac{\partial u}{\partial t}(x,0) = u^1(x), \quad \theta(x,0) = \theta^0(x), \quad \frac{\partial \theta}{\partial t}(x,0) = \theta^1(x), \quad (2)$$

with specified functions u^0, u^1, θ^0, θ^1. Boundary conditions are problem-specific. In all computational experiments reported in this paper mechanical boundary conditions are either specified stress or specified displacement:

$$s(0,t) = s_1(t), \quad s(L,t) = s_2(t), \quad \text{or} \quad u(0,t) = u_1(t), \quad u(L,t) = u_2(t); \quad (3)$$

thermal boundary conditions are those of specified heat flux

$$\frac{\partial \theta}{\partial x}(0,t) = \bar{\theta}_1(t), \quad \frac{\partial \theta}{\partial x}(L,t) = \bar{\theta}_2(t), \quad (4)$$

where functions $s_i(t)$ (or $u_i(t)$) and $\bar{\theta}_i(t)$, $i = 1, 2$ are given. The model (1)–(4) will be used here as the basis for our computational analysis of the phase transformation dynamics and hysteresis phenomena in a shape memory alloy rod.

The coupling of thermal and mechanical fields is a key component of the models we deal with in this paper. The description of phase transformations with the model (1)–(4) is based on a non-convex free energy function, which leads to a non-monotone load-deformation curve [15]. This idea, often attributed to van der Waals, was further developed theoretically by Landau and in the context of shape-memory-alloys was pioneered by Falk [13]. The model (1)–(4) incorporates the Helmholtz free energy in the Landau-Devonshire form. Note, however, that there are several avenues of improving model (1)–(4). One lies with the improvement of the Landau-Devonshire phenomenological model used in the derivation of (1). As it was noted in [7, 4] a "slight" change in this function, such as the account for or omitting of the viscous or coupled stresses, thermal memory terms, etc may require different mathematical arguments in the analysis of the well-posedness of the model and in the construction of numerical schemes used for its solution. Indeed, strictly speaking the free energy function should be derived on the basis of statistical arguments [16] and the idea of van der Waals developed further by Landau is a possible approximation of this function, sufficient for a wide range of applications. Another important avenue of improving model (1)–(4) lies with constitutive models. It is not the purpose of this paper to move along any of these avenues. Instead, by using (1)–(4) we show that it is possible to capture main features of the dynamics of phase transformations and hysteresis phenomena at a low computational cost with the methodology proposed. Furthermore, the methodology we developed earlier (e.g., [5]) allows to derive *systematically* centre manifold approximations of more complicated 3D models (in a sense discussed above, see also [17] and references therein) which then can be treated in a way similar to that described in this paper.

Our final remark in this section goes to the Landau-Devonshire-Ginzburg approximation for the free energy function which we have used in a number of computational experiments with an appropriately modified model (1)–(4). This approximation assumes the dependency of the free energy on a change of the curvature ϵ_x of the metallic lattice. The form of this dependency determines the coupled stress $\zeta = \zeta(\epsilon_x)$, an extra term in the free energy function, that typically takes the smoothing role of the viscous stress and simplifies the analysis of the mathematical model. The definition of this term varies in the literature with the most common taken to be a quadratic dependency $(\gamma/2)\epsilon_x^2$, known as the Ginzburg term

(γ is the Ginzburg coefficient). This term leads to the appearance of an additional term, γu_{xxxx}, in the first equation of system (1). With reported values of the Ginzburg coefficient ($\gamma \sim 10^{-10} - 10^{-12}$) this term showed little influence on the dynamics of shape-memory alloys in the group of computational experiments we performed (see also [5]). However, we note that for the deformation-driven set of computational experiments the choice of the value for the Ginzburg coefficient can help in differentiating between rate-dependent and rate-independent hystereses (e.g., [18] and references therein).

3. Low-Dimensional Modelling of SMA Dynamics and Reductions to Differential-Algebraic Systems

In this section we highlight main steps in the numerical solution of (1)–(4). As we mentioned in the previous section, the phenomenon of phase transitions in shape memory alloys is fairly complicated and models aiming at capturing the macroscopic response of SMA-based systems will be continuously re-examined with improved thermodynamic constitutive equations, allowing to bring into light new additional effects. Therefore, it is important to develop a general methodology that on the basis of complex models that describe the whole range of complicated effects, often of little practical interest, would allow to derive simpler models which are able to capture the main features of the dynamics by using a subset of the possible modes, so-called critical modes [19]. One specific example of this approach has recently been considered by the authors in [5]. First, in the spirit of [14] we used some physically justified assumptions to reduce the number of required parameters for Cu-based shape memory alloys from 32 (in the general 3D case) to 10. These parameters for $\mathtt{Cu_{14}Al_3Ni_{83}}$ (see Ref. [14]) were used in the the construction of a low dimensional model for shape-memory-alloy dynamics. Using the computer algebra package **REDUCE** such a model was derived from the 3D Falk-Konopka model [14] for modelling a shape-memory-alloy slab that has a very large extent in the x-direction compared to its thickness ($2b$) in the y-direction ($-b < y < b$). The essential dynamical behaviour of the slab was determined effectively by a subset of all possible modes. This is a key idea of a quite general methodology arising from centre manifold theory [20, 21, 19, 22, 5, 23].

The development of low-dimensional models such as the one described above is very important for this field of mechanics. Since one has to deal with a hierarchy of models for shape memory alloy dynamics [3], center manifold techniques provide an effective methodology to derive new improved models in this hierarchy. Moreover, there is a fundamental link between center manifold theory and normal forms and it is well known that these two methodologies provide very powerful tools in studies dynamics of complex oscillatory systems arising in different areas of mechanics and its applications [23]. The theory of center manifold originated from works of Pliss goes back to more than 30 years (see [20] and references therein), its comprehensive account was given in a book by Carr [21], but only during recent years with advances in computer algebra the theory has undergone a substantial development for several important areas of applications, including SMA [19, 22, 5].

The important point to note is that once a low-dimensional model is derived the procedure of its reduction to a system of differential-algebraic equations puts us in a situation similar to that considered in the present paper. The accuracy of such low-dimensional models can be improved systematically [19], hence the control of accuracy in the solution of the original problem is determined by the differential-algebraic solver. Let us explain this in some detail.

In [5], starting with the general 3D Falk-Konopka model we constructed the model with respect to the amplitudes of the critical modes, U_i, V_i $(i = 1, 2)$ and Θ' based on the existence of a low-dimensional invariant manifold upon which these amplitudes evolve slowly [19, 20, 23]. These amplitudes were chosen as y-averages of u_i, $i = 1, 2$ (displacements in x- and y- directions respectively), v_i, $i = 1, 2$ (velocities in x- and y- directions respectively) and $\theta' = \theta - \theta_0$ with θ_0 taken $300°$ K. Then, a model for the longitudinal unforced dynamics of $\mathtt{Cu_{14}Al_3Ni_{83}}$ shape-memory-alloy slab can be derived systematically, up to the arbitrary order of accuracy [19, 22]. Note that for shape memory alloy applications we have used $\mathcal{O}\left(E^p + \partial_x^q(\cdot) + \vartheta^r\right)$ to characterised the error of low dimensional models obtained by neglecting all terms involving $\partial_x^{\beta_1} E^{\beta_2} \vartheta^{\beta_3}$ such that $\beta_1/p + \beta_2/q + \beta_3/r \geq 1$, where $E = \|\mathbf{U}_x\| + \|\mathbf{V}_x\|$ and $\vartheta = \|\Theta'\|$. We note that once such a low dimensional model is derived its treatment can be based on the same numerical procedures as the treatment of model (1)–(4) considered in this paper. The particular model (in terms of the amplitudes) for the longitudinal dynamics on the invariant manifold derived in [5] had the accuracy $\mathcal{O}\left(E^8 + \partial_x^4(\cdot) + \vartheta^4\right)$. Then, the displacements and temperatures were found with error $\mathcal{O}\left(E^5 + \partial_x^{5/2}(\cdot) + \vartheta^{5/2}\right)$. Models with higher order accuracy are obtained with the same methodology described in [5]. Using computer algebra, a low-dimensional model can be easily modified to take into account mechanical and/or thermal forcing as well as higher order terms, then can be reduced to a system of differential-algebraic equations, and solved in a way similar to the solution of the problem described here as an example.

Indeed, consider system (1). This system is a strongly nonlinear system of partial differential equations that couples hyperbolic and parabolic modes of the dynamics in a unified whole. However, if we simplify the system by assuming $\tau_0 = \mu = \nu = 0$, it can be seen that the main terms responsible for the coupling phenomenon are $k_1\theta\dfrac{\partial u}{\partial x}\dfrac{\partial v}{\partial x}$ and $\dfrac{\partial}{\partial x}\left(k_1\dfrac{\partial u}{\partial x}(\theta - \theta_1)\right)$ in the first and the second equation, respectively. As shall be seen in Section 4, these terms provide the basis for the analysis of the phase transition mechanism.

Several numerical procedures have been reported in the literature for the solution of systems of PDEs describing shape-memory-alloy dynamics (see, for example, Ref. [11, 24] and references therein). Our approach is different from those previously reported. The main idea of our approach is a transformation of the problem (1)–(4) into a system of differential-algebraic equations with respect to (u, v, θ, s). Then we solve this system by using one of the backward difference integration algorithms developed in **MATLAB** (e.g., [5]). In particular, we reduce the original system to form $\tilde{\mathtt{f}}(\mathtt{t}, \mathtt{y}, \mathtt{y}') = \mathtt{0}$ with given vector function $\tilde{\mathtt{f}}$, and the integration procedure, starting from column-vector `y0` at time `t0` and finishing at time `tfin`, returns the solution at all times in `tspan` $= [\mathtt{t0}, \mathtt{t1}, ..., \mathtt{tfin}]$. The time step and `tspan`, responsible for error management, and the Jacobian of $\tilde{\mathtt{f}}$ are provided by the user to compute $[\mathtt{f}, \mathtt{k}, \mathtt{m}] = \mathtt{func}(\mathtt{t}, \mathtt{y}, \mathtt{y}')$. Note that both `k` and `m` may be given as sparse matrices. A three-level procedure has been developed to guarantee the convergence of the algorithm. For all computational experiments reported in the next section the first level of the algorithm with second-order accurate spatial differences on staggered grids (`dae2`) is sufficient. The other two levels of the algorithm (based on fourth-order accurate scheme `dae4` and multi-step method `dae4o`) are used to confirm the result obtained with `dae2`. The developed **MATLAB** code is simple, robust and easy to implement.

Taking into account the above assumptions the transformed system for all computational

experiments described in Section 4 has the following form

$$\begin{cases} \dfrac{\partial u}{\partial t} &= v, \\ \rho\dfrac{\partial v}{\partial t} &= \dfrac{\partial s}{\partial x} + F, \\ C_v\dfrac{\partial \theta}{\partial t} &= k\dfrac{\partial^2\theta}{\partial x^2} + k_1\theta\dfrac{\partial u}{\partial x}\dfrac{\partial v}{\partial x} + G, \\ s &= k_1(\theta-\theta_1)\dfrac{\partial u}{\partial x} - k_2\left(\dfrac{\partial u}{\partial x}\right)^3 + k_3\left(\dfrac{\partial u}{\partial x}\right)^5. \end{cases} \tag{5}$$

The term $\dfrac{\partial u}{\partial x} = \epsilon$ in (5) is the linearised strain that plays the role of the order parameter in the Landau theory. The initial and boundary conditions for this model are problem-specific and will be defined in the next section. All computational experiments reported here were performed for a $Au_{23}Cu_{30}Zn_{47}$ rod of the length $L = 1$cm. For the $Au_{23}Cu_{30}Zn_{47}$ material all necessary parameters were first specified by Y. Murakami (see ref. in Falk [13]). In the context of system (5) we use (see also Ref. [11])

$$k = 1.9\times10^{-2}\text{cmg/(ms}^3\text{K)}, \quad \rho = 11.1\text{g/cm}^3, \quad C_v = 29\text{g/(ms}^2\text{cmK)}, \quad \theta_1 = 208\text{K},$$

$$k_1 = 480\text{g/(ms}^2\text{cmK)}, \quad k_2 = 6\times10^6\text{g/(ms}^2\text{cmK)}, \quad k_3 = 4.5\times10^8\text{g/(ms}^2\text{cmK)}.$$

4. Phase Transition Dynamics under Different Thermomechanical Conditions

Due to a wide range of industrial applications and associated challenging applied mechanics and mathematics problems, the control of phase transitions in shape memory alloys has recently become a topic of considerable interest [8]. In this section we investigate different options for the control of shape memory alloys, including stress-boundary control, distributed heating and their combination. Special attention is given to the computational analysis of hysteresis.

I. First, we apply the methodology developed in the previous sections to modelling stress induced phase transitions. It is known that the stress-induced phase transition exhibits a hysteresis, provided that we have thermodynamic barriers to prevent an equilibrium phase transition [13]. In the following two computational experiments the role of these barriers is played by the boundary stress chosen as the main control variable.

I.1. Consider initial conditions (e.g., [12])

$$u(x,0) = \epsilon_0 x, \quad v(x,0) = 0, \quad \theta(x,0) = 230, \tag{6}$$

and choose $\epsilon_0 = 0.106051$, so that the rod initially in martensitic phase M_+. For the given initial temperature this state is stable and we need to change thermomechanical conditions of the rod to induce a phase transition (for such a low temperature the same is also true for M_- martensitic phases).

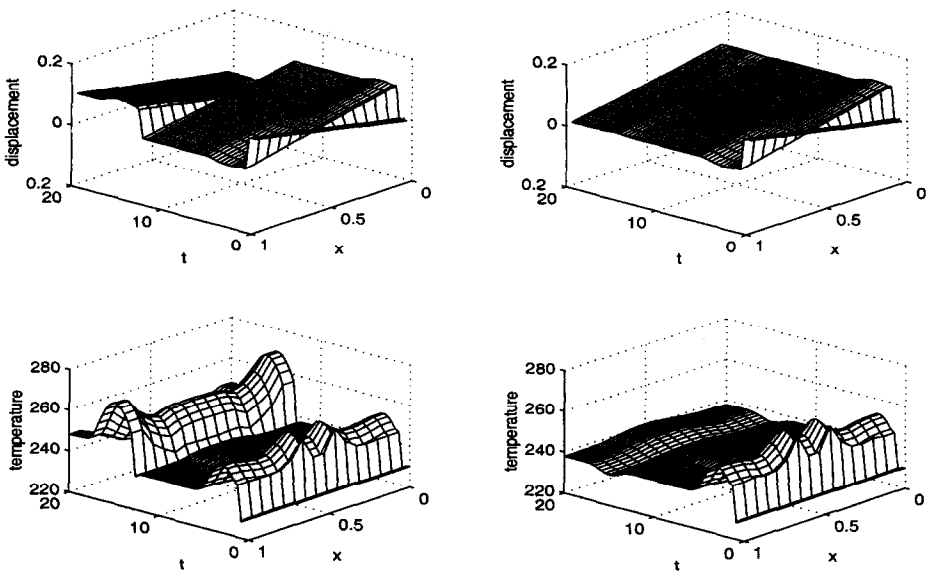

Figure 1: SMA responses to dynamic loadings: (a) stress induced phase transition where the tensile load exceeds the yield limit (left); (b) absence of thermodynamic barriers to prevent an equilibrium phase transition where the tensile load is less than the yield limit (right).

We assume no distributed loading (i.e. $F = G = 0$). Instead, for the first 6 ms we load the rod at the boundaries (which are assumed to be thermally insulated) with the compressive load $-7000\sin^3(\pi t/6)\,\mathrm{g/(ms^3cm)}$. Then, for the next 6 ms we do not apply any force, and for the next 6 ms after that we apply a tensile load $7000\sin^3(\pi t/6)\,\mathrm{g/(ms^3cm)}$. Therefore, we have the following boundary conditions on $x = 0$ and L:

$$\frac{\partial\theta}{\partial x} = 0\,, \quad s = \begin{cases} -7000\sin^3(\pi t/6), & 0 \le t \le 6, \\ 7000\sin^3(\pi t/6), & 12 \le t \le 18, \\ 0, & \text{otherwise.} \end{cases} \tag{7}$$

During the initial period, observe the phase transformation $M_+ \to M_-$ in Fig. 1 (the upper-left plot). Then, observe the appearance of two regions with a slight increase/decrease in displacement (upward and downward "humps"). These regions demonstrate *thermomechanical coupling effects* between the two phases in the period when the temperature pattern changes (see the lower-left plot in Fig. 1). After a while, one observes that these regions vanish and we have only the M_- phase which is in stable equilibrium. Finally, observe a reverse phase transformation $M_- \to M_+$ (due to the tensile load) according to a pattern which is analogous to that described above. The behaviour of this type is typical for ferroelastic materials. When subjected to low initial temperatures, shape memory alloys do not produce an intermediate austenite phase under the above thermomechanical conditions.

I.2. In the previous example we saw that after the transformation $M_+ \to M_-$ takes place, the reverse transformation $M_- \to M^+$ is possible under fairly high tensile loading exceeding

the yield limit. If the last condition is not satisfied, the rod would remain in the M_- phase. This is demonstrated by the next computational experiment, where the tensile loading was set 10 times lower than in the previous example:

$$s = \begin{cases} -7000\sin^3(\pi t/6), & 0 \le t \le 6, \\ 700\sin^3(\pi t/6), & 12 \le t \le 18, \\ 0, & \text{otherwise.} \end{cases} \tag{8}$$

All other conditions remained the same as in computational experiment I.1. The effect of thermomechanical coupling (after the transition $M_+ \to M_-$) is observed only for a short period of time. It results in small perturbations visible on Fig. 1 (the upper-right plot) as the regions with two "humps". After that the rod returns to the M_- stable equilibrium.

The situation will not qualitatively change if we keep a constant load (say, $s = 100$) for all the times when the compressive/tensile load at the boundary is absent, i.e. when

$$s = \begin{cases} -7000\sin^3(\pi t/6), & 0 \le t \le 6, \\ 700\sin^3(\pi t/6), & 12 \le t \le 18, \\ 100, & \text{otherwise.} \end{cases} \tag{9}$$

The almost-linear behaviour of displacements and only small variations in temperature (the lower-right plot in Fig. 1) on the second stage of this computational experiment suggests that the rod exhibits elastic properties under the given thermomechanical conditions.

With spatial and temporal steps $0.06\bar{6}$ cm and 9.26×10^{-4} ms respectively, computations I.1 and I.2 take on average 10–11 minutes to complete on a Digital Alpha 255 station (300 MHz).

I.3. Hysteresis phenomena are important in our understanding of dynamic response of SMA elements, but to quantify these phenomena remains a difficult task. Models for hysteresis are under close attention in the theoretical development of new mathematical models for complex phenomena (e.g., [25] and references therein) and practical applications in mechanics [26, 27, 18]. The non-convexity and the non-linear thermal dependency of the free energy function, used in the derivation of mathematical models such as (1)–(4), play key roles in the understanding of hysteresis-type phenomena. Indeed, in the general case these characteristics imply non-monotone stress-stress relationships (or load-deformation diagrams) which depend on the temperature change in a complicated nonlinear manner. We explore such situations below.

Hysteresis phenomena intrinsic to shape memory alloys are often characterised by different types of load-deformation diagrams (e.g., [16]), and in what follows we use this idea developed further in [10]. In particular, we start from the original configuration by considering again the case of mechanical loading in the low-temperature regime. The initial conditions for this computational experiment are chosen so that we start with two M_+ and one M_- martensites:

$$\theta^0 = 220\,, \quad u^0 = \begin{cases} 0.11869x, & 0 \le x \le 0.25, \\ 0.11869(0.5 - x), & 0.25 \le x \le 0.75, \\ 0.11869(x - 1), & 0.75 \le x \le 1, \end{cases} \quad v^0 \equiv u^1 = 0. \tag{10}$$

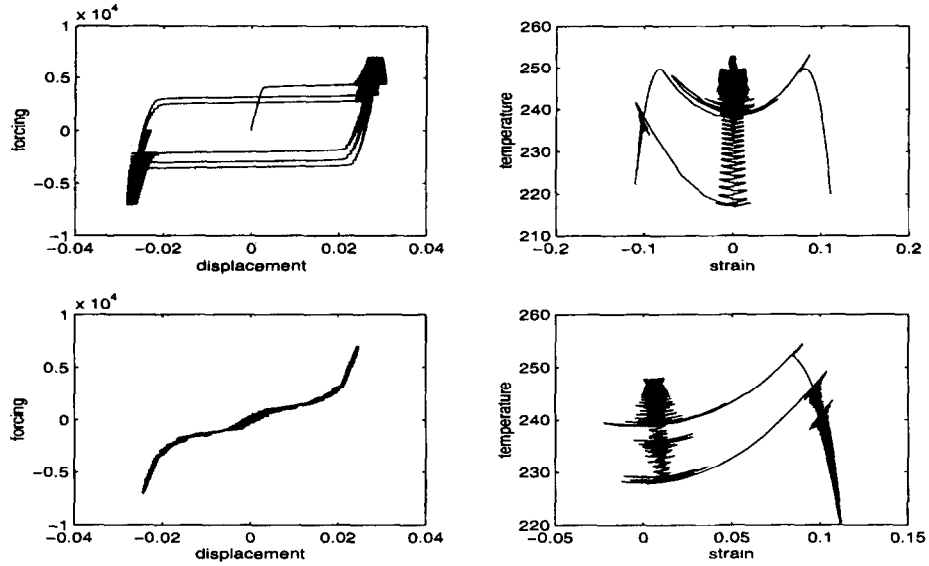

Figure 2: Mechanically and thermally induced hystereses, as observed for time-varying loading (11) at fixed spatial grid point $n_h = n/2 - 3$, where n is the total (even) number of intervals in space.

Then, in the absence of thermal loading ($G = 0$), by adding time-varying distributed mechanical loading

$$F = 7000 \sin^3\left(\frac{\pi t}{2}\right) \text{ g/(ms}^3\text{cm)} \tag{11}$$

and looking at fixed spatial grid point $n_h = n/2 - 3$ we plot u as function of F (in plots presented in Fig. 2 $n = 16$). Note that we do not need boundary stresses to demonstrate hysteresis with the computational model applied here, and hence we use pinned-end mechanical boundary conditions ($u = 0$), supplemented by $\dfrac{\partial \theta}{\partial x} = 0$. Such mechanical boundary conditions are somewhat artificial, because it is not easy to maintain them in practice, but the example itself is quite instructive since one can think of a rod with fixed ends whose oscillations are induced by applied time-varying force (11). Since under these thermomechanical conditions shape-memory-alloys behave like a ferroelastic material, one may expect a hysteresis loop to be observed [16, 10]. This phenomenon is clearly demonstrated by the upper left plot on Fig. 2.

I.4. Under intermediate-temperature conditions, shape-memory alloys behave like pseudoelastic materials. In this case, in spite of the difference in loading/unloading stress-strain curves, the mechanical loading does not lead to a residual strain [13].

In our next computational experiment we start from the martensitic state M_+ given by initial conditions $u^0 = 0.11869x$, $v^0 = 0$, and $\theta^0 = 270$. The thermal and mechanical distributed loading are the same as in computational experiment I.3, but now we use realistic mechanical boundary conditions by applying stress at the thermally insulated boundaries

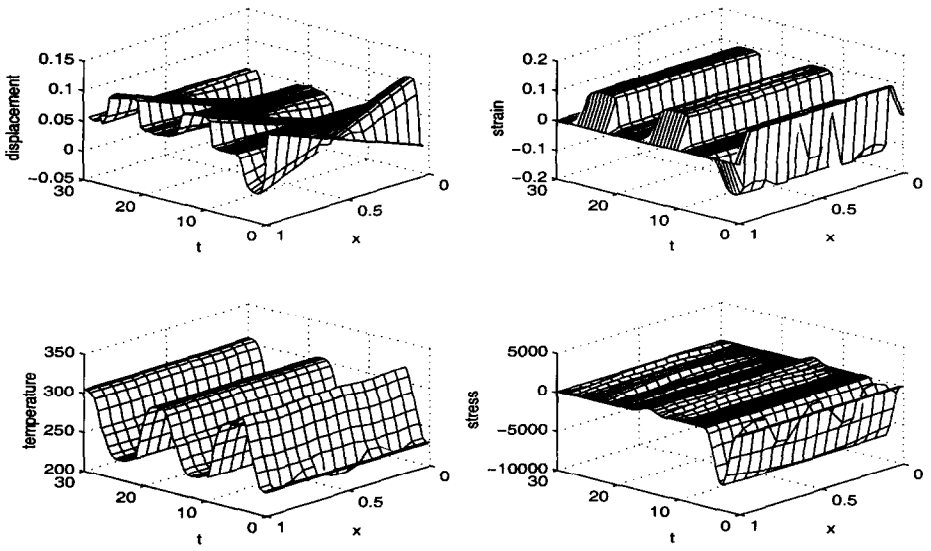

Figure 3: Temperature controls thermodynamic barriers allowing phase transitions even if the tensile load is less than the yield limit.

according to the following rule

$$s = \begin{cases} -1000\sin^3(\pi t/6), & 0 \le t \le 6, \\ 0, & \text{otherwise}, \end{cases} \qquad \frac{\partial \theta}{\partial x} = 0. \tag{12}$$

The given temperature is on the border of the "pseudoelastic" range and the two symmetric loops, that are typical for these thermomechanical conditions, are very small (see the lower-left plot on Fig. 2). Further increase in temperature leads to the complete disappearance of hysteresis since in this case shape-memory-alloys start to behave like elastic materials.

II. Temperature induced phase transitions are of fundamental importance in SMA applications. One of the major reasons for that lies with the fact that the purely mechanical control of phase transitions demonstrated above may not be always efficient. In the next series of computational experiments we show how to control this process by temperature. More precisely, we explore the range of temperature for which on cooling the formation of martensite starts; and conversely, the range of temperature, for which on heating, the formation of austenite starts. The driving force for this type of transition is the difference between the free energies of both phases. We control this difference by controlling the distributed heating/cooling pattern.

II.1. Consider our last computational experiment where we were unable to produce a phase transition with the given loading pattern. Let us keep the stress on the boundary such that (9) is satisfied and all other conditions, except for the distributed thermal loading, remain the same as in computational experiment I.2. The distributed heating/cooling used is

$$G = 375\sin^3(\pi t/6)\ \mathrm{g/(ms^3cm)}\,. \tag{13}$$

Then, after the initial switch $M_+ \to M_-$ (due to insufficiently low initial temperature), we observe phase transitions $M_- \to A$, then $A \to M_+$, $M_+ \to A$ etc (see Fig. 3). The hyperbolic features of this transitions expressed in superposed elastic vibrations are demonstrated by the stress plot presented in the lower-right plot on Fig. 3. This computational experiment demonstrate clearly that in those cases when the mechanical load alone is not sufficient to induce the phase transition in the rod, we can effectively use distributed heating/cooling to control the phase transition process.

Two concluding computational experiments are aimed at the description of hystereses in thermally-induced phase transformations.

II.2. Two symmetric martensites are taken as the initial state for the next computational experiment, namely

$$u^0 = \begin{cases} 0.11869x, & 0 \le x \le 0.5, \\ 0.11869(1-x), & 0.5 \le x \le 1, \end{cases} \quad v^0 = 0\,, \quad \theta^0 = 220\,. \tag{14}$$

In this computational experiment we assume constant distributed loading of $F = 500\mathrm{g}/(\mathrm{ms}^3\mathrm{cm})$ and thermal distributed loading $G = \dfrac{375}{2}\pi \sin^3\left(\dfrac{\pi t}{6}\right) \mathrm{g}/(\mathrm{ms}^3\mathrm{cm})$. First, we assume the same boundary conditions as in computational experiment I.3. In a way similar to that example (see also [10]), we look at fixed spatial grid point $n_h = n/2 - 3$, and plot s as function of time-varying temperature (in all plots presented in Fig. 2 $n = 16$). The temperature-strain plot, presented on the right-upper plot of Fig. 2, demonstrates temperature-induced transformations between austenite and martensites. Observe that these transformations are approximately symmetric with respect to the sign of strain.

II.3. Finally, we assume no mechanical distributed loading ($F = 0$). We start from an M_+ martensitic state defined by initial conditions $u^0 = 0.11869x$, $v^0 = 0$, and $\theta^0 = 220$. Boundary conditions now are those of stress-free $s = 0$ and insulated ends $\dfrac{\partial \theta}{\partial x} = 0$, while the distributed thermal loading is assumed to follow the same pattern as in computational experiment II.2. The lower-right plot of Fig. 2 gives the temperature-strain curve of the phase transformation between M_+ and A states.

With spatial and temporal steps 0.0625 cm and 6.67×10^{-4} ms respectively, computations for hysteresis reported here take on average 33–36 minutes to complete on a Digital Alpha 255 station.

Finally, we sketch our explanations of the overall shape of the temperature-strain curves in computational experiment II.2 and II.3 by allowing a simple approximate analysis used at our recent SMS Symposium presentation. Let us assume that the strain varies in time but is more-or-less uniform over the rod. This allows us to claim that $\dfrac{\partial u}{\partial x} \approx \varsigma f(t)$ with a certain constant coefficient ς (see Fig. 4 for a schematic representations of the transformation $M_+ \to A$). We integrate this relationship (assuming the mean displacement to be zero)

$$u = \varsigma x f(t) \quad \text{and, hence,} \quad v = \varsigma x \frac{\partial f}{\partial t}\,, \tag{15}$$

and then differentiate the result (15). We obtain that $\dfrac{\partial v}{\partial x} = \varsigma \dfrac{\partial f}{\partial t}$.

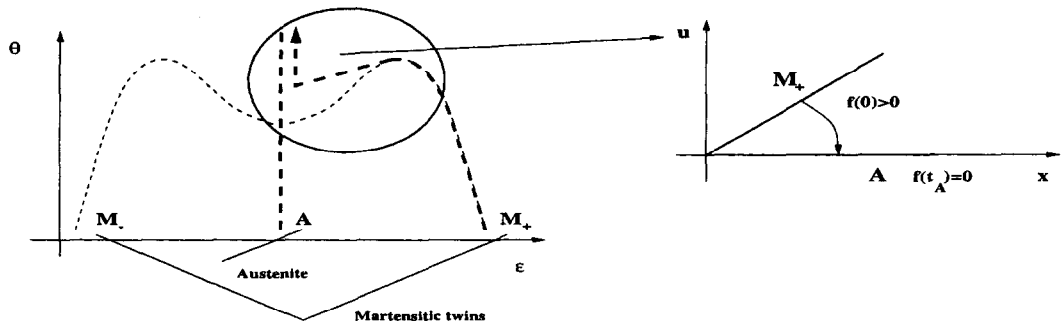

Figure 4: Schematic representations of thermally induced hystereses.

Note further that in the absence of diffusion ($k = 0$) when $\tau_0 = 0$ and $\mu = \nu = 0$, the thermal equation of system (1) can be simplified to

$$\frac{\partial \theta}{\partial t} = k_c \theta \frac{\partial u}{\partial x}\frac{\partial v}{\partial x}, \quad \text{where} \quad k_c = k_1/C_v. \tag{16}$$

Using the above representations for $\dfrac{\partial u}{\partial x}$ and $\dfrac{\partial v}{\partial x}$ in terms of the function f, from (16) we get that

$$\frac{1}{\theta}\frac{\partial \theta}{\partial t} = k_c \varsigma^2 f \frac{\partial f}{\partial t}. \tag{17}$$

Hence, taking into account that $f = \dfrac{1}{\varsigma}\dfrac{\partial u}{\partial x}$, an approximation to the strain-temperature relationship is derived directly from (17) as

$$\ln \frac{\theta}{\theta_c} = \frac{k_c}{2}\varsigma^2 f^2 \quad \text{or} \quad \ln \frac{\theta}{\theta_c} = \frac{k_c}{2}\left(\frac{\partial u}{\partial x}\right)^2, \tag{18}$$

where θ_c is a constant. The last relationship confirms the parabolic shape of the temperature-strain curves in the transitions from martensites to austenites as depicted on the right-hand side plots of Fig. 2.

5. Concluding Remarks

Approximations to models describing the dynamics of shape memory alloys can be systematically derived via the application of centre manifold theory [3, 4, 5]. Such approximations can be treated efficiently with numerical procedures based on the reduction of such PDE-based approximations to differential-algebraic equations. In this paper we considered a model derived from the Landau-Devonshire phenomenology and demonstrated effectiveness of our numerical procedures in capturing all main features of the dynamics of phase transitions and hysteresis phenomena. We applied such numerical procedures to the computational analysis of stress- and temperature-induced transitions in a large Cu-based shape memory alloy rod. The analysis of non-monotone stress-strain relationships that depend on the temperature change in a complicated nonlinear manner has also been performed.

The geometry of hysteresis loops as a function of temperature requires further investigations. The width of hysteresis may often be determined by an additional term which is responsible for the interfacial energy and when this term vanishes the phase transition may occur reversibly. Models that are derived using free energy functions that incorporate interfacial energy contributions and take into account the influence of mechanical and thermal dissipations (such as the latent heat) may prove to be helpful. It seems natural to apply the methodology based on centre manifold techniques to such models.

Finally, we note that, strictly speaking, the models presented in this paper are applicable only for single crystals. A much more complex task is to describe the dynamic of composite heterogeneous materials with SMA components considered as polycrystalline materials. Some such components may be formed as a mixture of elastic and viscoelastic materials in a way similar to other thermoviscoelastic materials (e.g., [28]), and the resulting models are extremely difficult to analyse. To find centre manifold approximations to such models present a challenge for future work.

Acknowledgments:

The authors were supported by Australian Research Council small grant 17906. The financial support of the University of Southern Queensland is also gratefully acknowledged.

References

[1] V. Birman, Review of mechanics of shape memory alloy structures, *Appl. Mech. Rev.* **50**, 629–645, 1997.

[2] G.A. Maugin, *Nonlinear Waves in Elastic Crystals*, Oxford University Press, Oxford, N.Y., 1999.

[3] R.V.N. Melnik, A.J. Roberts, and K.A. Thomas, Mathematical and numerical analysis of Falk-Konopka-type models for shape memory alloys, *Int. J. of Differential Equations and Applications*, **1A(3)**, 291–300, 2000.

[4] R.V.N. Melnik and A.J. Roberts, Approximate models of dynamic thermoviscoelasticity describing shape-memory-alloy phase transitions, in *New Methods in Applied and Computational Mathematics*, Eds.: R.V.N. Melnik, D. Stewart, S. Oliviera, 17-32, Austral. Nat. Univ., Canberra, 2000.

[5] R.V.N. Melnik, A.J. Roberts, and K.A. Thomas, Computing dynamics of copper-based SMA via centre manifold reduction of 3D models, *Computational Materials Science*, **18**, 255–268, 2000.

[6] H. Benzaoui et al, Experimental study and modelling of a TiNi shape memory alloy wire actuator, *Journal of Intelligent Material Systems and Structures*, **8**, 619-629, 1997.

[7] J. Sprekels, Global existence for thermomechanical processes with nonconvex free energies of Ginzburg-Landau form, *Journal of Mathematical Analysis and Applications*, **141**, 333-348, 1989.

[8] N. Bubner, J. Sokolowski, and J. Sprekels, Optimal boundary control problems for shape memory alloys under state constraints for stress and temperature, *Numer. Funct. Anal. and Optimiz.*, **19**, 489-498, 1998.

[9] R.S. Anderssen, I.G. Gotz, and K.-H. Hoffmann, The global behavior of elastoplastic and viscoelastic materials with hysteresis-type state equations, *SIAM J. Appl. Math.*, **58(2)**, 703-723, 1998.

[10] O. Klein, Stability and uniqueness results for a numerical approximation of the thermomechanical phase transitions in shape memory alloys, *Advances in Mathematical Sciences and Applications (Tokyo)*, **5(1)**, 91-116, 1995.

[11] M. Niezgodka and J. Sprekels, Convergent numerical approximations of the thermomechanical phase transitions in shape memory alloys, *Numer. Math.*, **58**, 759-778, 1991.

[12] H.W. Alt, K.-H. Hoffmann, M. Niezgodka, and J. Sprekels, A Numerical Study of Structural Phase Transitions in Shape Memory Alloys, *Department of Mathematics, University of Augsburg*, **90**, 1985.

[13] F. Falk, Model free energy, mechanics, and thermomechanics of shape memory alloys, *Acta Metallurgica*, **28**, 1773-1780, 1980.

[14] F. Falk and P. Konopka, Three-dimensional Landau theory describing the martensitic phase transformation of shape-memory alloys, *J. Phys.: Condens. Matter.*, **2**, 61-77, 1990.

[15] I. Muller and H. Xu, On the pseudo-elastic hysteresis, *Acta Metall. Mater.*, **39(3)**, 263-271, 1991.

[16] M. Bornert and I. Muller, Temperature dependence of hysteresis in pseudoelasticity, in *Free Boundary Value Problems*, Eds.: K.-H. Hoffmann and J. Sprekels, 27-35, Birkhauser, 1990.

[17] D. Bernardini, On the macroscopic free energy functions for shape memory alloys, *J. of the Mechanics and Physics of Solids*, **49**, 813–837, 2001.

[18] N. Bubner, G. Mackin, and R. Rogers, Rate dependence of hysteresis in one-dimensional phase transitions, *Computational Materials Science*, **18**, 245–254, 2000.

[19] A.J. Roberts, Low-dimensional modelling of dynamics via computer algebra, *Computer Physics Communications*, **100**, 215–230, 1997.

[20] V.A. Pliss G.R. and Sell, Approximation dynamics and the stability of invariant sets, *J. of Differential Equations*, **149**, 1–51, 1998.

[21] J. Carr, Applications of Centre Manifold Theory, Springer, Berlin, 1981.

[22] A.J. Roberts, Computer algebra derives correct initial conditions for low-dimensional dynamical models, *Computer Physics Communications*, **126**, 187–206, 2000.

[23] S.-N. Chow, W. Liu, and Y. Yi, Center manifold of invariant sets, *J. of Differential Equations*, **168**, 355–385, 2000.

[24] K.-H. Hoffmann and J. Zou, Finite element approximations of Landau-Ginzburg's equation model for structural phase transitions in shape memory alloys, M^2AN, **29(6)**, 629-655, 1995.

[25] A. Visintin, Hyperbolic equations with hysteresis, *C.R. Acad. Sci. Paris, Series I*, **332**, 315–320, 2001.

[26] N. Bubner, Landau-Ginzburg model for a deformation-driven experiment on shape memory alloys, *Continuum Mech. Thermodyn.*, **8**, 293–308, 1996.

[27] H.-T. Bank et al, Modeling of nonlinear hysteresis in elastomers under uniaxial tension, *J. of Intel. Material Systems and Structures*, **10**, 116–134, 1999.

[28] H.I. Ene, M.L. Mascarenhas and J. Saint Jean Paulin, Fading memory effects in elastic-viscoelastic composites, M^2AN, 31(7), 927-952, 1997.